microbial biotechnology

Open Access

Label-free proteomic dissection on *dptP*-deletion mutant uncovers *dptP* involvement in strain growth and daptomycin tolerance of *Streptomyces roseosporus*

Dan Zhang,[1,†] Xixi Wang,[1,†] Yang Ye,[1] Yu He,[1] Fuqiang He,[1] Yongqiang Tian,[2] Yunzi Luo[3] and Shufang Liang[1]***

[1]*State Key Laboratory of Biotherapy and Cancer Center, Collaborative Innovation Center for Biotherapy, West China Hospital, Sichuan University, Chengdu, 610041, China.*

[2]*Key Laboratory of Leather Chemistry and Engineering, Ministry of Education and College of Light Industry, Textile and Food Engineering, Sichuan University, Chengdu, 610065, China.*

[3]*Key Laboratory of Systems Bioengineering (Ministry of Education), School of Chemical Engineering and Technology, Tianjin University, Tianjin, 300072, China.*

Summary

Daptomycin (DAP) is a novel microbial lipopeptide antibiotic synthesized by the DAP biosynthetic gene cluster *dpt* of *Streptomyces roseosporus (S. roseosporus)*. *DptP* gene locates upstream of *dpt* and confers DAP resistance to *Streptomyces ambofaciens (S. ambofaciens)*. So far, the biological functions of *dptP* gene for *S. roseosporus* growth are still completely uncovered. We performed label-free quantification proteomic dissections with loss- and gain-of-function experiments to decipher *dptP*-involved functions. Deletion of *dptP* gene activated energy metabolism and metabolism of secondary metabolites pathways and enhanced the transcription levels and protein abundance of key members of the *dpt* cluster. Whereas *dptP* deletion inhibited transport/signal transduction and drug resistance pathways and protein abundance of cell division-relative proteins, subsequently decreased mycelia cell growth rate. *S. roseosporus* strain with *dptP* deletion was more sensitive to DAP treatment compared to the wild type. In contrast, overexpression of *dptP* gene decreased transcription levels of DAP biosynthetic genes and enhanced growth rate of *Streptomcyes* strain upon elevated culture temperature and DAP supplementation. Taken together, *dptP* gene contributes to *Streptomcyes* primary growth under elevated temperature and DAP treatment, whereas it plays negative roles on metabolism of secondary metabolites and transcription of DAP biosynthetic genes.

Received 5 July, 2020; accepted 7 December, 2020.
For correspondence *E-mail zizi2006@scu.edu.cn; Tel. +13 008 152730; Fax +028-85 502 796.
For correspondence **E-mail: yunzi.luo@tju.edu.cn, Tel.18608011365; Fax +86-22-27403389.
[†]These authors contributed equally to this study.
Microbial Biotechnology (2021) **14**(2), 708–725
doi:10.1111/1751-7915.13736
Funding Information
This work was financially supported by the grants from Sichuan Science & Technology Program (2020YFH0094), Chengdu Science & Technology Program (2020-GH02-00056-HZ) and the Health Commission of Sichuan Province (17ZD045).

Introduction

A lot of microbial natural products are significant drug candidates for treatment of bacterial infections, viral infections and other diseases (Butler *et al*., 2014; Li *et al*., 2019). *Streptomycetaceae* family produces various druggable secondary metabolites (Xu and Wright, 2019; Zhu *et al*., 2011), including anti-infection antibiotics. As reservoirs for natural products, *Streptomyces* strains are widely engineered to improve the yield of target products (Ke and Yoshikuni, 2019; Tao *et al*., 2018). Daptomycin (DAP), a bioactive lipopeptide synthesized by a non-ribosomal peptide synthetase (NRPS) gene cluster *dpt* (GenBank: AY787762.1) of *S. roseosporus* (Fig. 1A) (Debono *et al*., 1987; Miao *et al*., 2005), has high-efficiency antibacterial activities against Gram-positive bacteria (Akins and Rybak, 2001; Robbel and Marahiel, 2010). The trademark of DAP drug, namely Cubicin ®) (Cubist Pharmaceuticals Inc., Lexington, MA, USA), was approved for treatment of skin and skin structure infections induced by Gram-positive bacteria (Arbeit *et al*., 2004; Ye *et al*., 2019).

The subunits of NRPS of DAP are encoded by three core biosynthetic genes, including *dptA*, *dptBC* and *dptD*. The upstream transport-related genes *dptM* and *dptN* encode ATP-binding and membrane spanning components of ATP-binding cassette (ABC) transporters (R.H., 2008). *DptE* and *dptF* play roles in coupling fatty acids to N-terminal Trp residue (Wittmann *et al*., 2008). The downstream regulatory genes *dptR1* and *dptR2* and upstream regulatory gene *dptR3* are responsible for

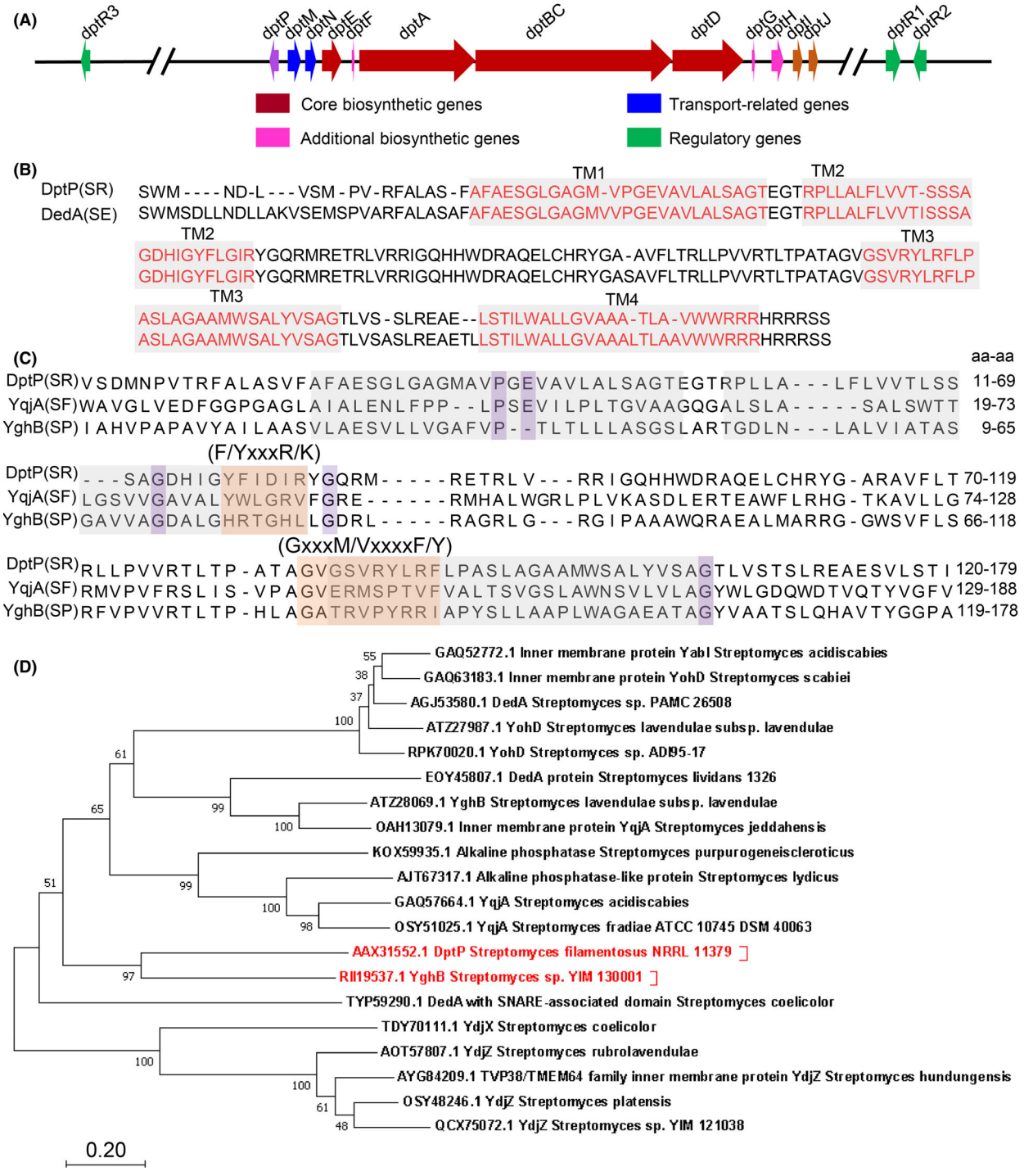

Fig. 1. Alignment comparisons of *dptP*-encoding DptP protein with DedA family proteins from other species.
A. The constitution of DAP biosynthetic gene cluster *dpt*. The *dptP* gene was presented in purple.
B. The amino acid similarity comparisons of *S. roseosporus* DptP with the DedA family protein of *S. exfoliatus*. Four transmembrane (TM) domains were highlighted in red font and grey background. SE: *S. exfoliates*.
C. Multisequence alignment for DptP from *S. roseosporus* and DedA family proteins from other species by MEGA software. The conserved motifs, F/YxxxR/K and GxxxM/VxxxxF/Y, were highlighted in orange background. Highly conserved glycine (G), acidic amino acids (E), basic amino acids (R) were highlighted in purple background. The TM domains were highlighted in grey background. SR: *S. roseosporus*. SF: *S. fradiae*. SP: *Streptomyces* sp. YIM 130001.
D. The phylogenetic tree analysis of *S. roseosporus* DptP and DedA family proteins from other *Streptomyces* species using MEGA software. Numbers on the branches are bootstrap values obtained from neighbour-joining method. Branch length represents the variation (genetic distance) of evolutionary branches as number. Scale bar indicates the branch length.

DAP biosynthesis (Wang *et al*., 2014; Zhang *et al*., 2015). The *dptP* gene locates upstream of the *dpt* gene cluster (Fig. 1A), and it is indicated to confer DAP resistance to *Streptomyces ambofaciens* (*S. ambofaciens*) (Alexander *et al*., 2004). Moreover, *dptP*-encoding protein is predicted to block the antibacterial activity of DAP and A54145 by directly interacting with acidic DAP for its basicity (Baltz *et al*., 2008; Baltz *et al*., 2005). However, there still lacks a comprehensive understanding of *dptP* functions. It is unclear whether and how *dptP* plays roles in biological processes excepting for DAP resistance in *Streptomyces* strains.

Proteomics technology contributes to new antibiotic discovery and pathway elucidation (Bordoloi *et al*., 2016; Machado *et al*., 2017). Protein levels are commonly correlated with the levels of metabolites (Gubbens *et al*., 2014; Chen *et al*., 2017). Thus, proteomics techniques based on mass spectrometry (MS) facilitate discoveries of gene clusters and pathway elucidations for valuable compounds. The label-free quantification (LFQ) is a liquid chromatography – tandem mass spectrometry (LC-MS/MS) based quantitative proteomics approach without high cost of the reagents and incomplete labelling (Zhu *et al*., 2010). Additionally, LFQ is suitable for rapid identification and quantitation of specific proteins in one group (Toymentseva *et al*., 2020). Thus, LFQ is widely applied to compare differences between two or among several groups.

In this study, we combined LFQ proteomics technology and CRISPR-Cas9 tool to further explore *dptP*-mediated multiple functions in *S. roseosporus*. *DptP*-induced changes in proteome profiling of *S. roseosporus* were identified by LFQ proteomics, which demonstrated *dptP*-encoding protein DptP and a series of altered strain proteins played positive roles in transport/signal transduction pathway and drug resistance, and negative roles in energy metabolism pathway and metabolism of secondary metabolites pathway. Furthermore, *dptP* was confirmed to contribute to growth tolerance upon elevated temperature and DAP accumulation through loss- and gain-of-function validations in *S. roseosporus*. Our results have supported and provided solid evidences to complement the previous conclusion obtained by Dr. Alexander (Alexander *et al*., 2004). We have applied LFQ proteomics in combination with CRISPR-Cas9 technologies to dissect biochemical functions of *dptP*. The strategies used in this report provide references for the follow-up study on other genes of *dpt* gene cluster and metabolic pathway optimization for *S. roseosporus*.

Results

Bioinformatics prediction of dptP-encoding protein

The *dptP*-encoding protein DptP with 206 amino acids (aa) shares a 91.75% sequence identity with the DedA family protein of *Streptomyces exfoliates* (accession no. WP_030556220.1) and contains 4 transmembrane domains (Fig. 1B). DedA family proteins consist of 8 members, including YqjA, YghB, YabI, YohD, YqaA, YdjX, YdjZ and DedA (Boughner and Doerrler, 2012), typically range from 200 to 250 aa and play roles in cell division, temperature sensitivity and drug resistance (Boughner and Doerrler, 2012; Doerrler *et al*., 2013; Kumar and Doerrler, 2015, 2014).

Considering DptP similarity with DedA family member, we compared the aa sequences of DptP protein with several DedA family proteins from other *Streptomyces* strains through alignment comparison. DptP shares 32.85% and 36.84% identities to the 228-aa YqjA of *Streptomyces jeddahensis* and 215-aa YghB of *Streptomyces* sp. YIM 130001 separately. DptP exhibits notable features of the DedA family proteins (Doerrler *et al*., 2013), including several highly conserved glycine residues and two prominent conserved sequence motifs, GxxxM/VxxxxF/Y and F/YxxxR/K (Fig. 1C) . Moreover, the evolutionary relationship indicates DptP of *S. roseosporus* and YghB of *Streptomyces* sp. YIM 130001 are clustered together in the phylogenetic tree (Fig. 1D), which indicates DptP is likely to be closer related to *Streptomyces* YghB protein in biological functions.

Deletion of dptP gene in S . roseosporus by CRISPR-Cas9

To further investigate the roles of *dptP* gene, most of the sequences of *dptP* gene from the 25th nucleotide to 556th nucleotide were deleted from *S. roseosporus* genome by an effective editing tool *Streptococcus pyogenes* CRISPR-Cas9 (Cobb *et al*., 2015; Wang *et al*., 2016), which resulted in a complete destruction of *dptP* gene and loss of its functions. Two spacers were selected to guide the CRISPR-Cas9. The *dptP*-deletion plasmid pCM2-*dptP* carried a sgRNA cassette with a configuration of gapdh (EL)-spacer 1-T7- gapdh (EL)-spacer 2-oop and an editing template (Fig. 2A). The double-strand break (DSB) caused by CRISPR-Cas9 was repaired by the editing template via homology-directed repair (HDR) (Fig. 2B). We randomly picked up 6 single colonies to validate *dptP* deletion via PCR. The efficiency of *dptP* deletion reached to 6/6 (Fig. 2C). PCR product from exconjugant 1 was subsequently sequenced, and the sequences were completely matched the upstream 248-bp and downstream 308-bp sequences near *dptP* (Fig. 2D, Fig. S1).

DptP-induced differential expression proteins were identified by LFQ proteomics

To have an insight into the roles of *dptP* gene on biosynthetic pathways, we detected the whole proteome

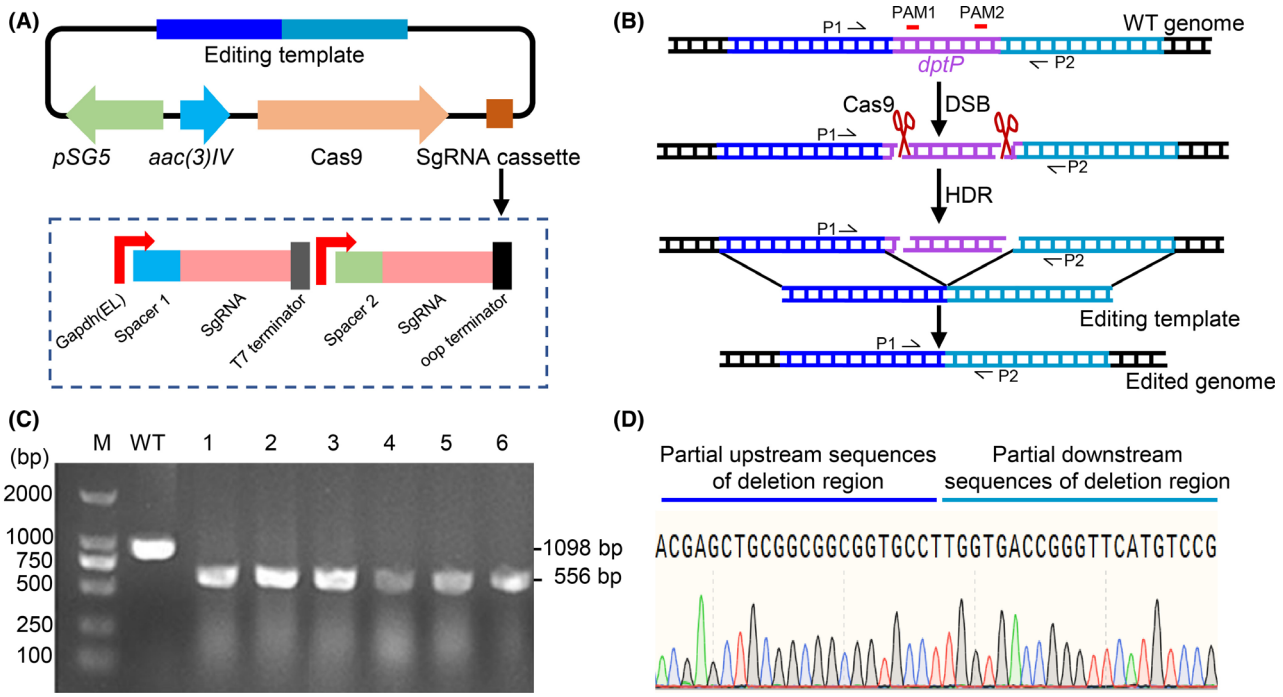

Fig. 2. CRISPR-Cas9-mediated *dptP* gene deletion in *S. roseosporus*.
A. The CRISPR-Cas9 system includes a *pSG5*, *acc(3)IV*, *Cas9*, sgRNA cassette and an editing template. The sgRNA cassette includes two spacers, including spacer 1 controlled by gapdh (EL) promoter and terminated by T7 terminator and spacer 2 controlled by gapdh (EL) promoter and terminated by oop terminator.
B. Schematic of CRISPR-Cas9-mediated *dptP* gene deletion. The editing template with a 931-bp upstream genome fragment and a 1035-bp downstream genome fragment near *dptP* is used to repair the double-strand break (DSB) cut by Cas9 via homology-directed repair (HDR). Primers P1 and P2 are used to perform PCR to check the deletion of *dptP* gene. Primer P1 locates upstream 248 bp far away from the deletion region. Primer P2 locates downstream 308 bp far away from the deletion region.
C. PCR evaluation for *dptP* gene deletion in *S. roseosporus*. Six single colonies (No.1-6) were randomly chosen to evaluate *dptP* deletion by PCR with primers P1 and P2. *DptP*-deletion strains generated 556-bp amplicons, and WT strain generated a 1098-bp amplicon.
D. DNA sequencing profiling of the 556-bp PCR fragment amplified from *dptP*-deletion strain. Partial upstream 248-bp sequences and downstream 308-bp sequences of deletion region were presented.

changes under *dptP* deletion using LFQ proteomics strategy based on LC-MS/MS with three technical replicates and three biological replicates (Fig. S2A). In total, 2313 proteins were identified in WT group, from which 2076 proteins were both identified in ΔdptP and WT group (Fig. S2B, Dataset S1A,B).

The wild-type (WT) *S. roseosporus* and *dptP*-deletion (ΔdptP) *S. roseosporus* showed no significant difference on growth rate at 30°C, which ensured the differential expression proteins were indeed induced by *dptP* loss instead of strain growth difference. Among the 2076 proteins identified in both strains, 101 proteins in the ΔdptP group showed significantly increased abundance (PSIA) (with a fold difference of $> +2.0$, $P < 0.05$), and 71 proteins showed significantly decreased abundance (PSDA) (fold difference of < -2.0, $P < 0.05$) (Fig. 3A, Dataset S1C,D). Additionally, 237 proteins were absent in the ΔdptP group due to *dptP* deletion (Dataset S1E). The multiscatter blot and the heatmap indicated a high degree of similarity among the biological replicates (Fig. S2C).

DptP-mediated differential expression proteins are involved in primary and secondary metabolisms

To further investigate *dptP*-mediated changes in biochemical molecular activities, we performed gene ontology (GO) analysis on all differentially expressed proteins (with a fold difference of < -2.0 or $> +2.0$, $P < 0.05$), including 101 PSIA (Dataset S1C), 71 PSDA (Dataset S1D) and 241 proteins absent in ΔdptP group (Dataset S1E). The top 4 activities for the PSDA, PSIA and AP proteins are involved in catalytic, binding, transporter and transcription factor activities (Fig. 3B–D), which indicates *dptP* is involved in both primary and secondary metabolisms of *S. roseosporus*.

KEGG pathway analysis of 172 proteins with statistically altered abundance (with a fold difference of < -2.0 or $> +2.0$, $P < 0.05$) was carried out to assess *dptP* involvement in metabolism pathways. Both PSIA and PSDA were involved in carbohydrate metabolism, energy metabolism, amino acid metabolism, transport/signal

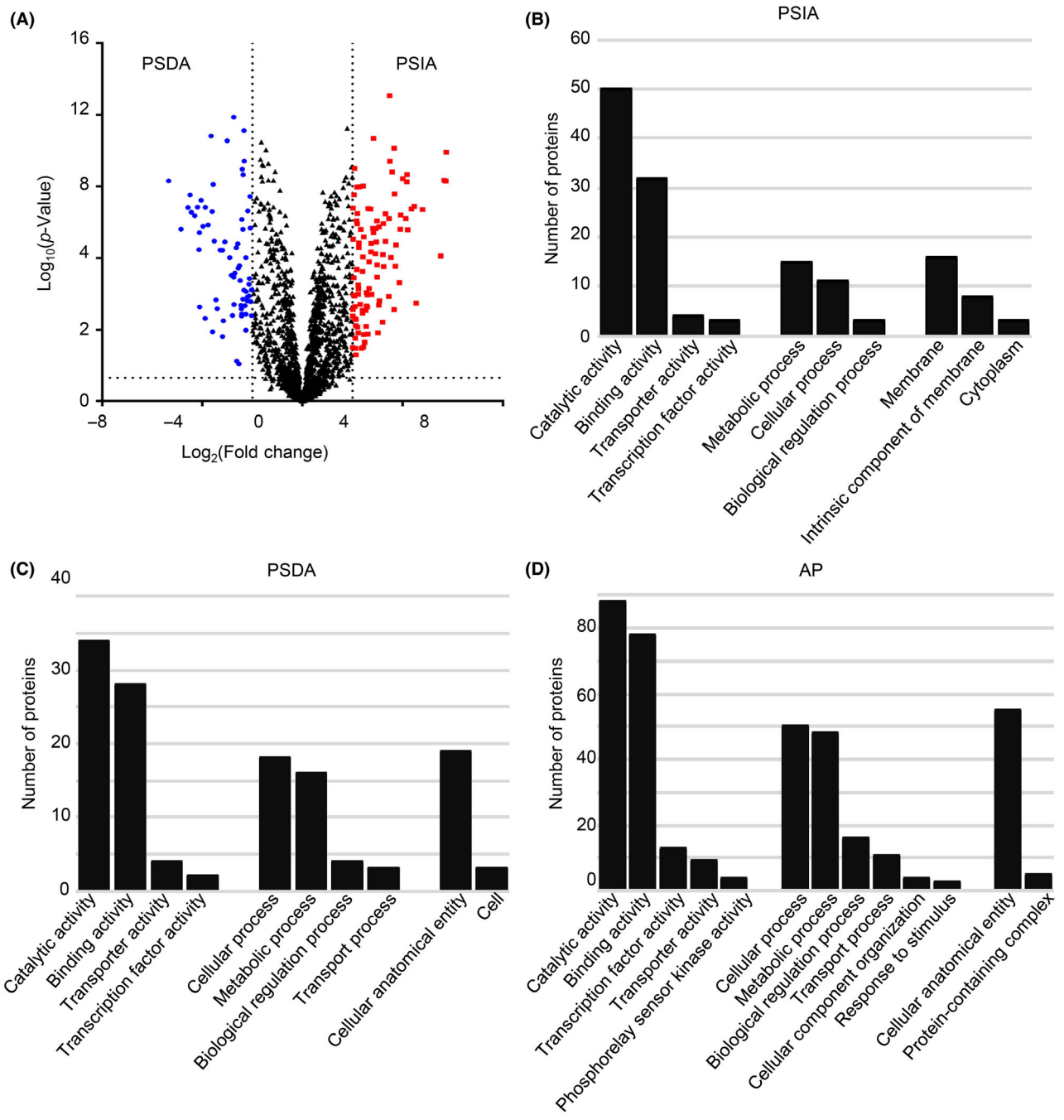

Fig. 3. Proteins with differential abundance between *S. roseosporus* WT and ΔdptP groups.
A. Volcano plot was generated from pairwise comparisons between WT and ΔdptP groups. Dashed lines represented the applied thresholds (ANOVA *P* value of < 0.05 and fold difference of > + 2.0 or < - 2.0). The proteins presented in blue, red or black indicated the PSDA, PSIA or the proteins with no significant difference.
B–D. GO analysis for the PSDA, PSIA and AP due to *dptP* deletion. PSDA: proteins with statistically decreased abundance, PSIA: proteins with statistically increased abundance, AP: absent proteins in ΔdptP group.

transduction, genetic information processing, lipid metabolism and nucleotide metabolism (Fig. 4A,B). According to the KEGG enrichment plots, the downregulated KEGG pathways mainly included carbohydrate metabolism, amino acid metabolism, transport/signal transduction, nucleotide metabolism, lipid metabolism and drug resistance (Fig. 4C). Moreover, the Zscores was introduced to quantitatively evaluate the *dptP*-involved pathways (Liu *et al.*, 2020), and similar conclusions were obtained as the KEGG analysis. For instance, the Zscore of

transport/signal transduction pathway was −7.29, which indicated a significant inhibition of this pathway due to *dptP* loss. On the contrary, several other pathways including energy metabolism, genetic information processing and metabolism of secondary metabolites were activated in response to *dptP* deletion (Fig. 4C). Notably, the Zscores of energy metabolism pathway and metabolism of secondary metabolites pathway were 5.76 and 4.89 respectively. This indicated energy metabolism and metabolism of secondary metabolites pathways seemed to be significantly activated since *dptP* loss. Generally, *dptP* plays positive roles in transport/signal transduction and drug resistance pathways, while it has negative roles in energy metabolism and metabolism of secondary metabolites pathways.

DptP protein locates in cell membrane of S . roseosporus

We constructed a Flag-tag-expression plasmid pSET152-*kasO*p*-*dptP* to introduce into *S. roseosporus* for observation of gain-of-function of *dptP* overexpression. The exogenous *dptP* gene within the *kasO*p*-*dptP*-Flag cassette was controlled by a constitutive strong promoter *kasO*p* (Wang *et al*., 2013) (Fig. 5A), which was designed to overexpress the C-terminally Flag-tagged DptP protein. The plasmid pSET152-*kasO*p*-*dptP* was confirmed to successfully insert into genome of *S. roseosporus* by PCR evaluation and sequencing (Fig. 5B–D, Fig. S2).

Subsequently, the transcription analysis showed that the relative expression level of *dptP* gene had a 468-fold enhancement in *dptP*-overexpressing *S. roseosporus* (abbreviate as OP strain in the following sections) (Fig. 5E). Meanwhile, the plasmid was also transferred to *S. ambofaciens* ATCC 23877, a DAP-susceptible actinomycete, to detect gain-of-functions of the exogenous *dptP* inducement (Fig. 5C). Total strain proteins were extracted to detect DptP protein using anti-Flag antibody, which indicated the DptP protein fused with C-terminal Flag was successfully expressed in *S. roseosporus* and *S. ambofaciens* (Fig. 5F). Moreover, we separated membrane proteins from the cytoplasm proteins in *S. roseosporus* according to cell membrane extraction procedures (Cheng and Li, 2014) to determine cellular localization of DptP protein. The exogenous DptP protein was mainly detected in the form of a 42-kDa dimer in membrane fractions (Fig. 5G), which supported our prediction that DptP protein is a membrane protein.

DptP *exhibits negative effects on gene transcriptional level for members of dpt gene cluster*

GO analyses revealed that a series of proteins were involved in catalytic (e.g. DptD), transporter (e.g. ammonium transporter) and regulator (e.g. AdpA, DptR2) activities. Among the PSIA enriched in catalytic activity, several proteins were responsible for the DAP biosynthesis. For instance, DptD, DptE and DptG showed notable increase of 3.49, 3.91 and 4.46 times respectively (Table 1).

To further elaborate the proteomic data, we compared the transcriptional changes of those gene members related to DAP biosynthesis in WT, ΔdptP and OP strains. Twelve genes were analysed, including biosynthetic genes (*dptA*, *dptBC*, *dptD*, *dptE*, *dptF*, *dptG*), transport-related genes (*dptM*, *dptN*) and regulatory gene (*dptR1*, *dptR2*, *dptR3*). As results, the transcription levels of all biosynthetic genes, including *dptA*, *dptBC*, *dptD*, *dptE*, *dptF* and *dptG* and regulatory gene *dptR2* were significantly increased due to *dptP* deletion (Fig. 6). On the contrary, the biosynthetic genes, *dptA*, *dptBC*, *dptD*, *dptE* and *dptF*, showed reduced transcription levels in response to *dptP* overexpression, while the transport-related *dptM* exhibited a markedly increased transcription level in OP strain (Fig. 6). All these data were consistent with the above proteomic conclusions that *dptP* deletion led to an activation of metabolism of secondary metabolites pathway and an inhibition of transport/signal transduction pathway.

DptP *gene is essential for strain growth under elevated temperature*

The proteome data showed that *dptP* deletion resulted in a significant decrease or loss of three proteins that were associated with cell division and DNA replication, including SepF1 (with a decreased level of 5.42 folds, $P < 0.05$), SepF3 and RecF (loss in ΔdptP group) (Dataset S1D,E, Fig. 7A-C). It is well known that DedA family protein YghB is essential for cell division at elevated temperature (Sujeet and William, 2014). Similar to the YghB within the phylogenetic tree relations (Fig. 1D), DptP was indicated to be important for strain growth.

To directly analyze the effects of *dptP* on strain growth, we measured the growth rates of WT, ΔdptP and OP strains grown at permissive 30°C and non-permissive 37°C. When grew at 30°C, the growth rates were similar among three groups (Fig. 8A). But the growth rates among the three groups showed significant differences after cultivation for 3 days at 37°C (Fig. 8B). Compared to the WT and ΔdptP strains, the OP strain was proven to survive and grow upon the unconventional cultivation temperature at 37°C. Namely, *dptP* gene is required for the growth rate of *S. roseosporus* at elevated culture temperature.

DptP contributes to mycelia growth of Streptomyces *under DAP exposure*

As we mentioned in our proteomic analysis, transport/signal transduction pathway and drug resistance

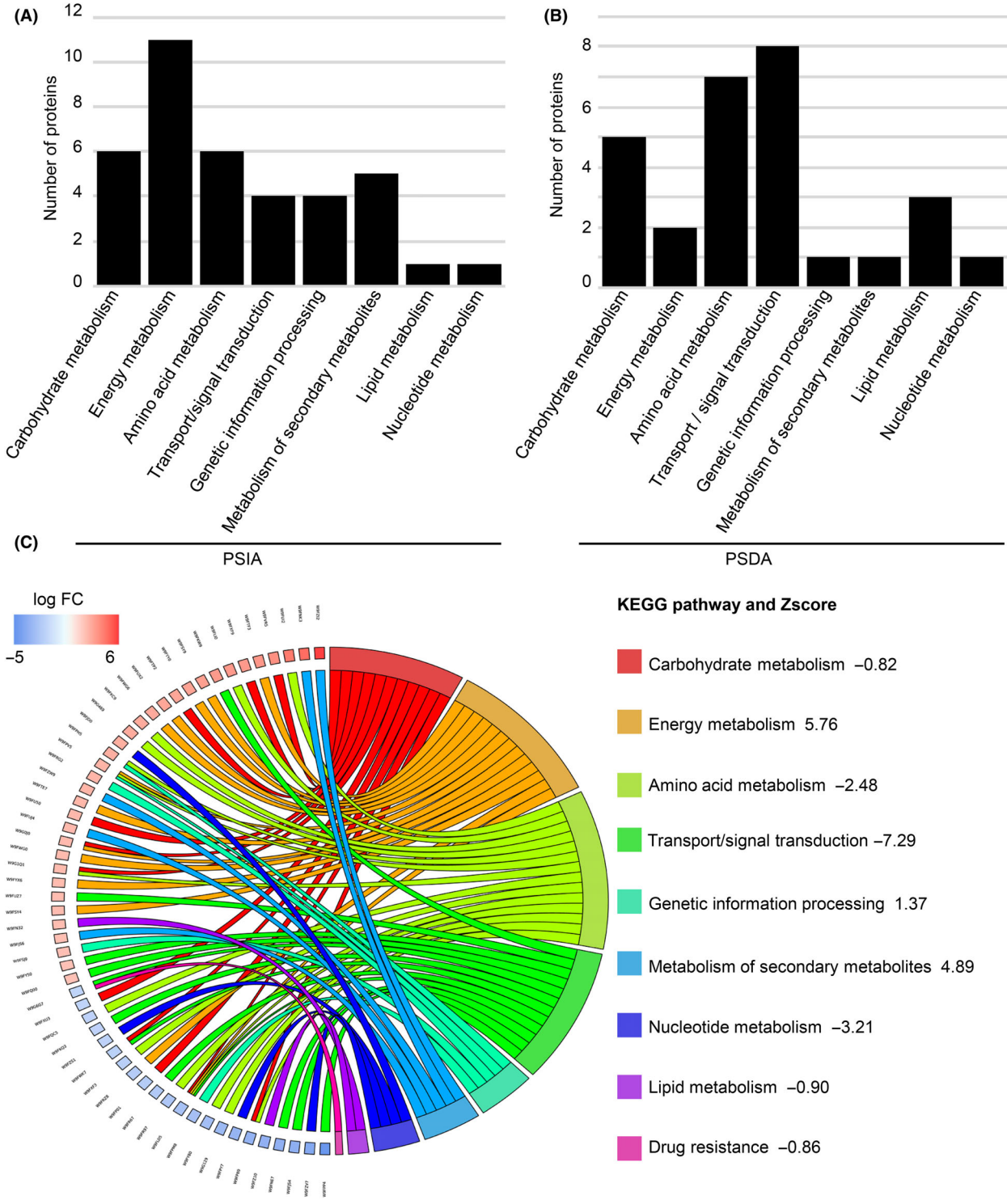

Fig. 4. KEGG analyses of all differential proteins.
A,B. KEGG enrichment for PSIA and PSDA. PSDA: proteins with statistically decreased abundance, PSIA: proteins with statistically increased abundance.
C. The KEGG enrichment plots for PSIA and PSDA. On the left side, the protein IDs and their corresponding values of $\log_2$FC were displayed in order from top to bottom. On the top, the values of $\log_2$FC are greater than 2 (red), and a larger $\log_2$FC indicates a greater difference of increased abundance. On the bottom, the values of $\log_2$FC are less than −2 (blue), and a smaller $\log_2$FC means a greater difference of decreased abundance. Nine significantly enriched pathways and their Zscores were shown on right side of the figure. When Zscore was less than zero, this pathway is more likely to be inhibited. Conversely, the pathway is more likely to be activated if Zscore value above zero.

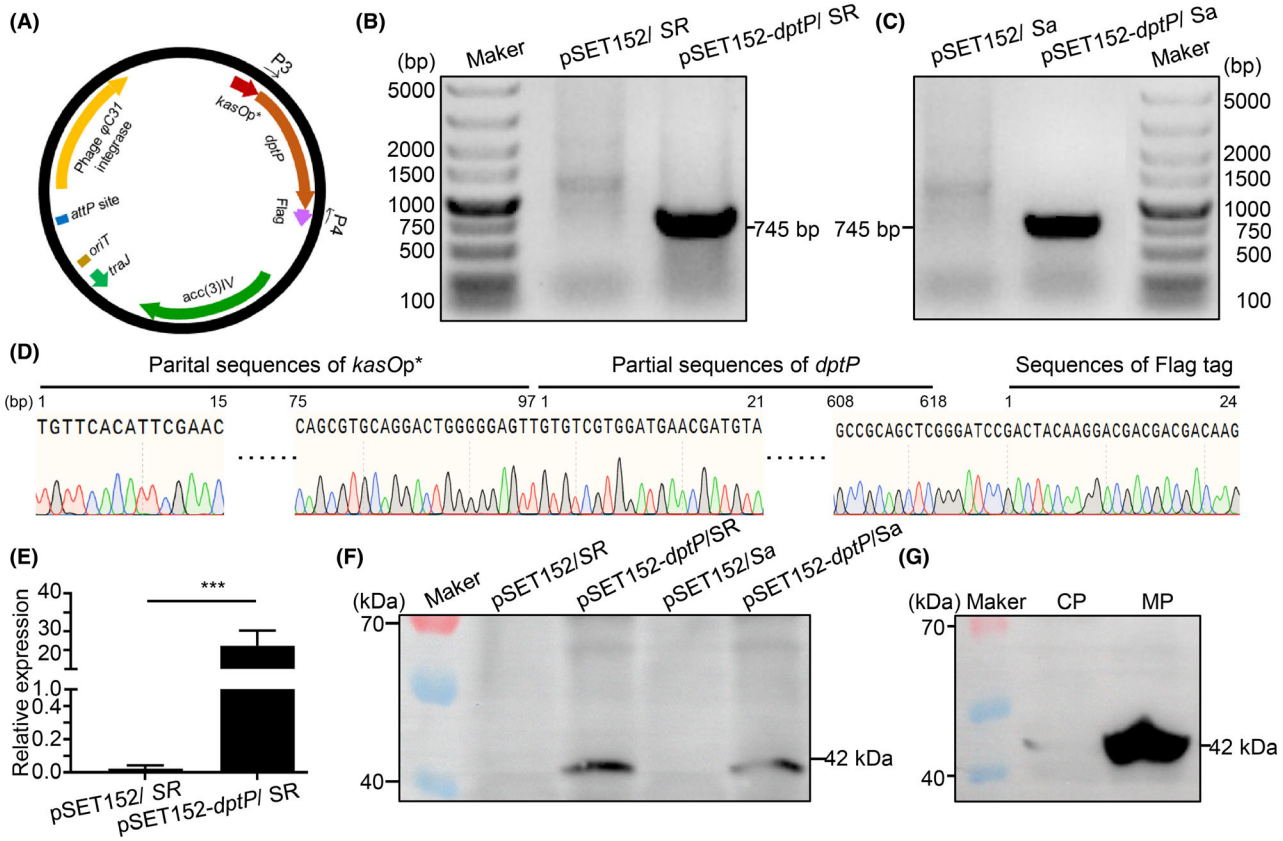

Fig. 5. Overexpression of *dptP* gene in *S. roseosporus*.
A. Schematic overview of pSET152-*kasO*p*-*dptP* plasmid. The elements of *oriT*, *traJ*, *φC31* and *attP* site help plasmid transfer to recipient host and integrate into host genome. The *kasO*p*-*dptP*-Flag cassette is composed of a constitutive strong promoter *kasO*p* and a *dptP* gene with a C-terminal Flag tag.
B,C. The integration of *kasO*p*-*dptP*-Flag cassette into the genome of *S.roseosporus* or *S.ambofaciens* by PCR evaluation. The 745-bp *kasO*p*-*dptP*-Flag fragment was amplified from the recombinant genome DNA of *S. roseosporus* or *S.ambofaciens* with primers P3 and P4. P3 locates in *kasO*p*, which is absent in WT or ΔdptP genome.
D. Sequencing data of the 745-bp product. Partial sequences of *kasO*p*, *dptP* gene and Flag tag were shown in the sequencing map.
E,F. Evaluation of expression level of exogeneous *dptP* gene (E) and its encoding Flag-tagging DptP protein (F) in *S. roseosporus* or *S. ambofaciens* by RT-qPCR and Western blot. SR: *S. roseosporus*; Sa: *S. ambofaciens*. pSET152/SR and pSET152/Sa represent the *S. roseosporus* strain and *S. ambofaciens* strain harbouring pSET152 respectively. pSET152-*dptP*/SR and pSET152-*dptP*/Sa represent the *S. roseosporus* and *S. ambofaciens* harbouring pSET152-*kasO*p*-*dptP* respectively. *** represents $P < 0.001$. The anti-Flag antibody was used to detect the Flag-tagging DptP protein by Western blot.
G. Cell localization of DptP protein. Membrane and cytoplasm fractions were detected using Western blot with anti-Flag antibody separately. The Flag-tagging DptP protein in the form of a 42-kDa dimer was detectable mainly in membrane fractions. MP: Membrane protein. CP: cytoplasm protein. The experiment was performed in triplicate.

pathway were significantly inhibited upon *dptP* deletion (Fig. 4C, Dataset S1C–E). Besides, previous work has shown that YghB is required for proton-motive-force drug resistance in *E. coli* (Sujeet and William, 2014). Thus, we also detected the roles of *dptP* against DAP tolerance. Wild-type *S. roseosporus* and *S. ambofaciens* had a growth arrest upon 0.5 and 0.2 mg ml^{-1} DAP incubation at 30°C respectively (Fig. 8C-D).

Furthermore, we compared the growth rates of the *dptP*-overexpression strain, *dptP*-deletion strain and their wild types under DAP treatment at 30°C. When exposure to 0.5 mg ml^{-1} DAP, the growth rate of ΔdptP strain presented a prominent reduce at 30°C compared to the WT strain since the 4th day (Fig. 8E). In contrast, the growth rate of *DptP*-overexpressing *S. roseosporus* strain (Fig. 8E) was improved since the 4th day compared to the growth rate of WT strain in MYG media containing 0.5 mg ml^{-1} DAP. To further have an insight into the changes on mycelia density, we measured the mycelia densities of *Streptomyces* species after DAP treatment for 6 days (density = number of cell forming units (C.F.U) ml^{-1}). Six days later, the mycelia were diluted to 10 000 times with MYG and spread on R2YE plates. There were 1.93 × 10^6 C.F.U. for WT at 30°C,

Table 1. Increased proteins resulted from *dptP* deletion in DAP biosynthetic gene cluster of *S. roseosporus*.

Protein IDs	Gene	Description	Difference	$-\log_{10}$ (*P* value)
W9FJV6	*dptA*	Peptide synthetase 1	+1.13	2.58
W9FJ42	*dptBC*	Peptide synthetase 2	+1.44	4.31
W9FJF2	*dptD*	Peptide synthetase 3	+3.49[a]	13.37
W9FNK8	*dptE*	Acyl-CoA ligase	+3.91[a]	9.61
W9FLE4	*dptF*	Probable acyl carrier protein	ND	
W9FJ44	*dptM*	Nodulation ABC transporter NodI	ND	
W9FJF4	*dptN*	Transport permease protein	ND	
W9FNK3	*dptG*	MbtH domain-containing protein	+4.47[a]	10.88
W9FLE0	*dptH*	LipE protein hydrolase	ND	
W9FJV4	*dptI*	SAM-dependent_MTases	+1.27	2.18
W9FJ39	*dptJ*	Tryptophan 2,3-dioxygenase	+1.08	0.08
W9FJ37	*dptR1*	HTH luxR-type domain-containing protein	ND	
W9FJE8	*dptR2*	HTH deoR-type domain-containing protein	ND	

ND, means not detected.
a. Significant change. + represents increased fold difference.

which were much more than those for ΔdptP and much less than those for OP (Fig. 8F). Similarly, *dptP*-overexpressing *S. ambofaciens* showed an increased growth rate and generated more C.F.U. than *S. ambofaciens* WT under 0.2 mg ml^{-1} DAP treatment (Fig. 8G-H). It was indicated that *dptP* gene contributed to mycelia growth under DAP exposure. Our results supported the previous work reported by Alexander (Alexander *et al*., 2004).

Discussion

It has been observed that biosynthetic genes, regulatory genes, transport-related genes are generally associated with DAP biosynthesis. In this study, we applied CRISPR-Cas9 and LFQ proteomics technologies with loss- and gain-of-function experiments to understand *dptP* functions on growth rate and metabolisms of *S. roseosporus*. We have confirmed that *dptP* gene plays positive roles on mycelia growth rate upon elevated temperature and DAP exposure. On the other hand, *dptP* exhibits negative roles on the transcription of gene members belonging to the *dpt* gene cluster.

Proteomics technology provides a promising exploitation in natural product discovery (Acharya *et al*., 2019), post-translational modification (Sun *et al*., 2020), elucidation of biosynthetic pathway (Bordoloi *et al*., 2016), even illustration of molecular mechanism response to a certain treatment (Guo *et al*., 2019). Specially, LFQ-based proteomic approach is simple and time saving for sample preparation and result analyses of MS identification and quantification. In this study, by LFQ proteomics approach, multiple *dptP*-mediated differential expression proteins of *S. roseosporus* were identified to be related to catalytic activity, binding, transmembrane transporter activity and regulator activity. Furthermore, KEGG pathway analysis demonstrated DptP protein and its related differential proteins were involved in inhibiting energy metabolism and metabolism of secondary metabolites pathways and activatting carbohydrate metabolism, amino acid metabolism, transport/signal transduction, nucleotide metabolism, lipid metabolism and drug resistance pathways. Except for *dptP* involvement in drug resistance that was reported in previous work (Alexander *et al*., 2004), proteomics approach provides more insights to biochemical functions of *dptP* gene.

To illustrate interactions of DptP with other *Streptomyces* proteins, Co-immunoprecipitation (Co-IP) in combination with MS identification was applied to screen the directly or indirectly interacting proteins. We enriched total membrane proteins by ultra-centrifuge (Cheng and Li, 2014), and enriched Flag-tagged DptP protein using anti-Flag antibody-coupled beads, subsequently. The protein complex of DptP protein and its interacting proteins were identified by LC-MS/MS. Three sugar transporters and one phosphoenolpyruvate carboxylase were identified in this assay, which was consistent with that these proteins showed decreased abundance after *dptP* deletion (Dataset S2A). These sugar transporters with decreased abundance may contribute to the decrease of glucose uptake and subsequently suppression of carbohydrate metabolism. Phosphoenolpyruvate carboxylase catalyses the reaction of phosphoenolpyruvic acid with carbon dioxide to produce oxaloacetic acid, and its decreased abundance is proposed to be involved in the inhibition of succinate dehydrogenase flavoprotein subunit, citrate synthase and succinate dehydrogenase iron–sulphur subunit, which are members of citric acid cycle (Dataset S2A). All these are responsible for the inhibition of carbohydrate metabolism. Additionally, the ABC transporter transmembrane subunit (W9FJ56) is a member of DAP cluster, its interaction with DptP protein seems to confer DAP resistance. Based on the potential DptP-interacting proteins identified by MS, further biochemical assays for elaborating the mechanisms will be performed in our following studies.

Among the PSIA enriched in catalytic activity, several proteins were responsible for the DAP biosynthesis (Table 1). DptD, DptE and DptG showed notable increase of 3.49, 3.91 and 4.46 times respectively. *DptD* gene encodes a non-ribosomal peptide synthetase, and *dptE* gene encodes an acyl-CoA ligase. *DptG* encodes a

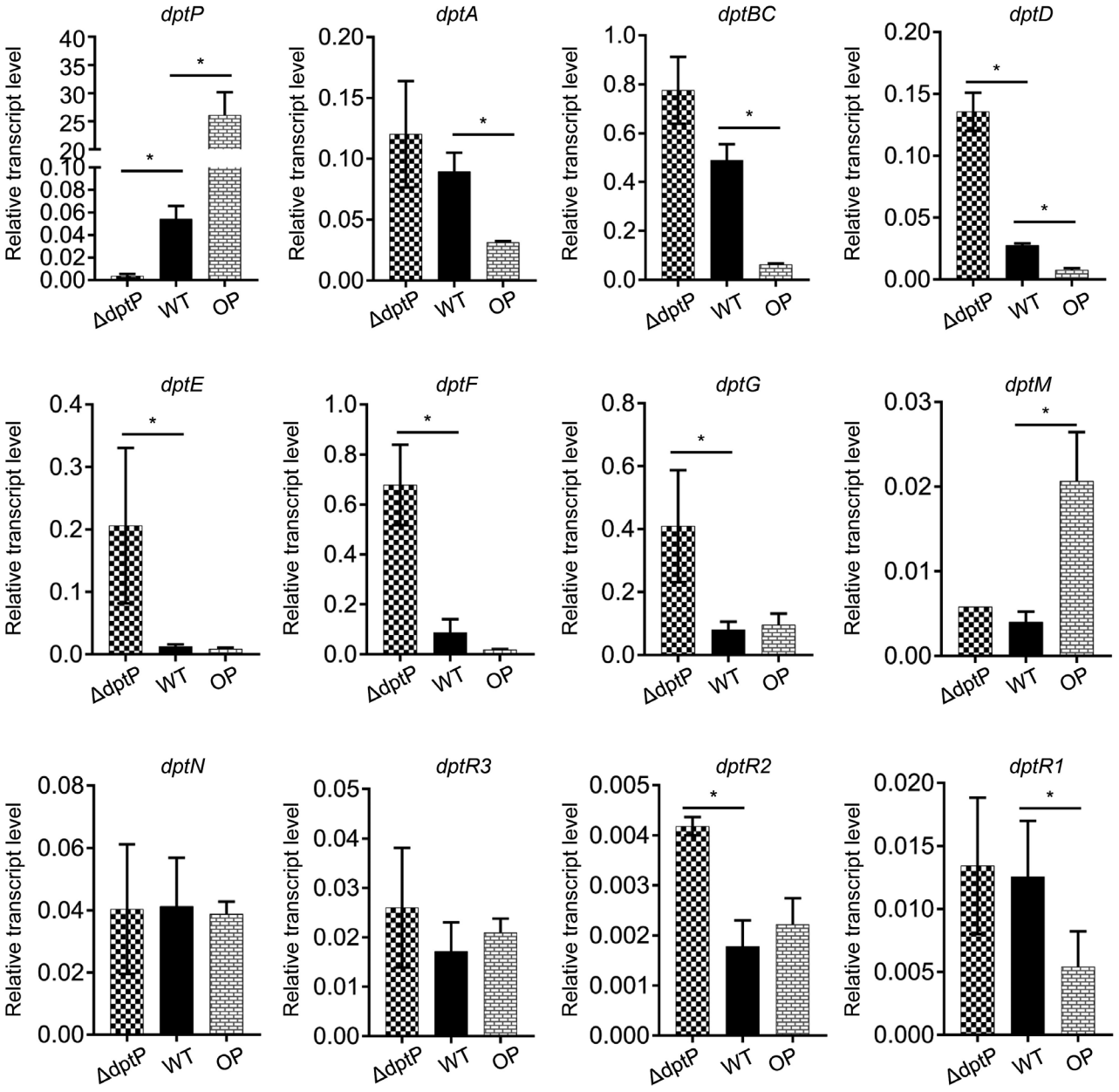

Fig. 6. Relative transcript levels of 12 gene members belonging to the *dpt* gene cluster. The relative transcript level of each gene was obtained after normalization against the internal reference *hrdB*. WT: wild-type *S. roseosporus*, ΔdptP: *dptP*-deletion *S. roseosporus*, OP: *dptP*-overexpressing *S. roseosporus*. The experiment was performed in triplicate.

MbtH domain-containing protein which plays prominent roles on NRPS-derived natural product biosynthesis by interacting with A domains of NRPS (Boll *et al*., 2011; Davidsen *et al*., 2013; Zolova and Garneau-Tsodikova, 2012). These three proteins are essential for the biosynthesis of DAP. Subsequent transcription analyses showed that *DptP* played negative roles on transcript levels of biosynthetic genes *dptD*, *dptE*, *dptF* and *dptG* (Fig. 6, Table 1). It is consistent with the KEGG analysis (Fig. 4C). Additionally, *dptP* deletion raised the transcription and protein levels of regulatory genes, such as *dptR2*, *adpA* (Fig. 6, Dataset S1C). These two genes are responsible for the DAP biosynthesis (Wang *et al*., 2014; Mao *et al*., 2015). We speculated the raising transcription and protein levels of regulatory genes contributed to the activation of biosynthesis of secondary metabolites. But how *dptP* deletion enhanced the transcription levels and protein abundance of the regulators is not clear so far, which needs further researches to explore it.

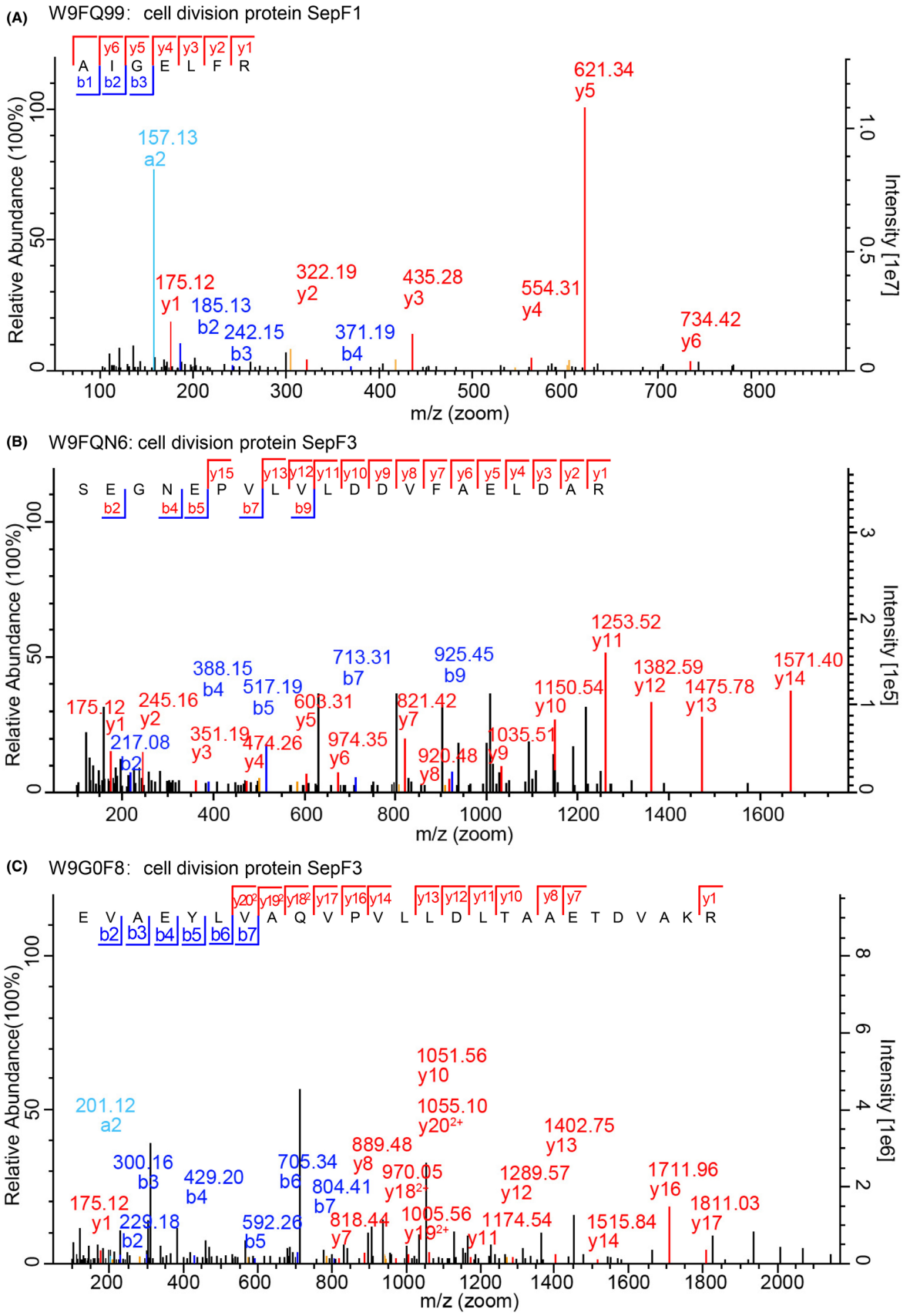

DptP-encoding protein shares a significant sequence identity with DedA family protein YghB. Further bioinformatic alignment showed there are several conserved motifs, such as GxxxM/VxxxxF/Y, F/YxxxR/K. These conserved motifs are related to the folding and stabilization of the proteins or higher oligomeric states (Keller and Schneider, 2013). Additionally, there are also acidic amino acids (E27 and E39) and basic amino acids (R117 and R123) within or in close to transmembrane spanning regions. These charged amino acids are important for the various proton-dependent secondary transporters, such as NhaA, MdtM (Fluman *et al*., 2012; Holdsworth and Law, 2012). What's more interesting, a recent report focusing on DedA family protein in *Burkholderia thailandensis* showed the membrane-embedded charged amino acids contributed to the colistin resistance (Panta *et al*., 2019). Thus, we supposed that the conserved amino acids of DptP contributed to the DAP tolerance in *S. roseosporus* and *S. ambofaciens*.

Previous work has identified that DedA family proteins are essential for bacterial growth of *E. coli* at 42°C (Boughner and Doerrler, 2012). Qualitative proteome data identified a significant decrease in abundance of cell division or replication proteins. Further experiments identified that *dptP* deletion was not favourable to the strain growth at elevated temperature, which was consistent to previous work. In this study, we provided a closer insight on the mechanism that disruption or mutation of DedA family protein arrests the strain growth by decreasing the protein levels of cell division- or replication-related proteins.

In conclusion, the proteomic and experimental data in this study provided better knowledge on characterization of *dpt* gene cluster. Our results also provided novel strategies to explore these unknown genes in biosynthetic gene clusters of valuable natural products. The strategy paves new avenues to study an unknown gene or gene cluster, even discover more broad-spectrum antibiotics.

Experimental procedures

Strains and plasmids

S. roseosporus NRRL 11379 was ordered from American Type Culture Collection (ATCC). *S. ambofaciens* was purchased from BeNa Culture Collection Company. *E. coli* ET12567/pUZ8002 and plasmid pSET152 were stored in State Key Laboratory of Biotherapy, Sichuan University. *E. coli* DH5α was purchased from Transgen Company (CD501-01, Transgen, China). The pCRISPomyces plasmid (pCM2) was friendly endowed by Prof. Huimin Zhao from University of Illinois, Urbana, USA.

Reagents

Restriction endonucleases including *Bbs*I (R3539S; NEB, Beverly, MA, USA), T4 DNA ligase (M0202S; NEB) and alkaline phosphatase calf intestinal (CIP) (M0290S; NEB) were ordered from New England Biolabs (Beverly, MA, USA). Genome DNA extract kit (D203, Tiangen, China) was purchased from Tiangen Company. WizardSV Gel and PCR Clean-Up System (A9281; Promega, Madison, WI, USA) were ordered from Promega. Iscript cDNA synthesis kit (170-8890; Bio-Rad, Hercules, CA, USA) and SYBR Green PCR 2 × Mix (172-5121; Bio-Rad) were ordered from Bio-Rad. Yeast extract, tryptone, NaCl, $MnCl_2$, $ZnSO_4$ and other reagents required for strain cultivation were purchased from Kelong (Chengdu, Sichuan, China). Soya flour was gifted from Jinan Huilong Company (Jinan, Shandong, China).

Plasmid construction

The *dptP*-deletion plasmid pCRISPomyces-*dptP* (pCM2-*dptP*) was constructed as following procedures (Cobb *et al*., 2015). Two protospacers, CCACACGATCGCGAGCGTGA and TACGGAGGCCAGCGCGAATC, were selected. The last 12-nt sequences of each protospacer plus 3-nt PAM sequences (15 nt total) were checked by BLAST to confirm their specificities. The configuration consisting of spacer1-sgRNAtracr-T7 terminator-gapdhp (EL)-spacer2 was synthesized and inserted into pCM2 plasmid by Golden Gate. Then, the repair template containing 931-bp upstream and 1035-bp downstream sequences near *dptP* was amplified from the genome DNA and inserted into *Xba*I site of spacer-containing plasmid.

The *dptP*-overexpression plasmid pSET152-*kasO*p*-*dptP* carried a *kasO*p*-*dptP*-Flag cassette, including a *kasO*p* promoter and a *dptP* gene fused with a C-terminal Flag tag. *DptP* gene was amplified from the genome of WT, and *kasO*p* promoter was amplified from template plasmid pkasOp (Wang *et al*., 2013). We

Fig. 7. MS/MS spectra of three *dptP*-deletion-mediated differential proteins related to cell division. The blue b ion indicates the ion reading from N-terminal to C-terminal of each peptide. The subscript number and bottom digits of b ion labelling the peak represent the number of N-terminal amino acids and their total molecular weight. Similarly, the red y ion indicates the ion reading from C-terminal to N-terminal. The subscript number and bottom digits of y ion present the number of C-terminal amino acids and their total molecular weight. The sequences of each peptide are calculated based on the b ions and y ions and their molecular weights. The letters on the top of each figure mean the single letter codes for the amino acids identified by MS. W9FQ99 (A) is a cell division protein SepF3. W9FQN6 (B) is a DNA replication and repair protein RecF. W9G0F8 (C) is a cell division protein SepF3.

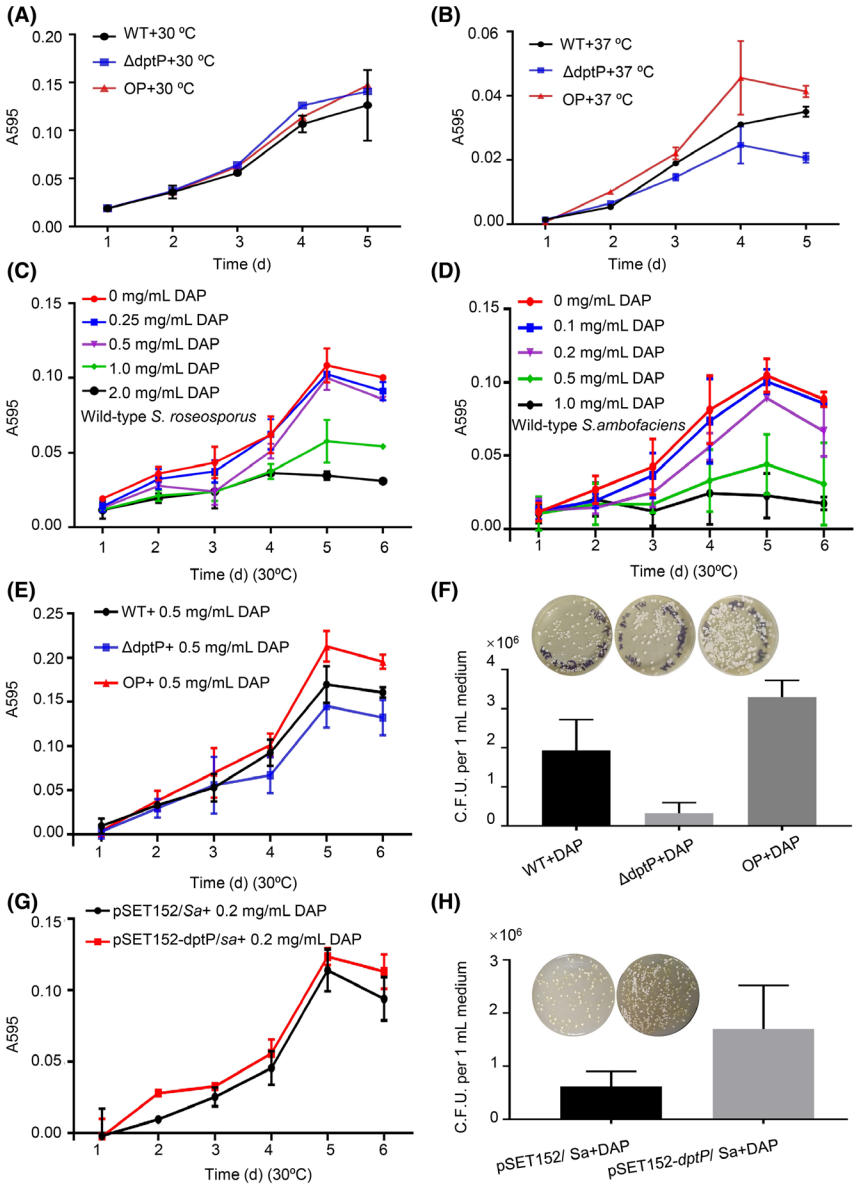

Fig. 8. Growth rates of *S. roseosporus* WT, ΔdptP and OP strains under different conditions were measured by diphenylamine colorimetric method.
A,B. Growth rates of *S. roseosporus* WT, ΔdptP and OP at 30 or 37°C. The spores were inoculated in MYG medium to culture at 30 or 37°C for 5 days.
C,D. Growth rates of *S. roseosporus* WT (C) and *S. ambofaciens* (D) upon 0.1-1mg/mL DAP incubation at 30°C. The absorbance at 595 nm (A595) was measured at the cultivation time of 1-6 d.
E–G. Growth rates of *S. roseosporus* WT, ΔdptP and OP and *S. ambofaciens* harbouring plasmid pSET152 or pSET152-*kasO*p*-*dptP* upon DAP incubation at 30°C. WT + DAP, ΔdptP + DAP, and OP + DAP: the wild-type, *dptP*-deletion and *dptP*-overexpression *S. roseosporus* were treated with 0.5 mg ml^{-1} DAP respectively. pSET152/*Sa* + DAP and pSET152-dptP/*Sa* + DAP: *S. ambofaciens* strains harbouring plasmid pSET152 or pSET152-*kasO*p*-*dptP* were treated with 0.2 mg ml^{-1} DAP.
F–H. Densities of the strains upon DAP treatment for 6 days at 30°C. Density = number of C.F.U. ml^{-1}. The culture for each *Streptomyces* strain from (E) or (G) at incubation time of 6 days was diluted and streaked on M-ISP4 plate, and grown at 30°C for 3–4 days respectively. Then, the C.F.U. presented on each plate was counted. The experiment was performed in triplicate.

constructed the plasmid by introducing *kasO*p*-*dptP*-Flag cassette into the *BamHI* and *XbaI* sites of pSET152 plasmid (Bierman *et al.*, 1992) via one step assembly (C114; vazyme, Nanjing, Jiangshu, China). All primers and plasmids were summarized in Dataset S3A,B.

Strain cultivation

E. coli strains were cultured in Luria–Bertani (LB) medium at 37°C. *S. roseosporus* NRRL 11379 and *S. ambofaciens* ATCC 23877 were cultivated in MYG media

(10 g l^{-1} malt extract, 4 g l^{-1} yeast extract and 4 g l^{-1} glucose) at 30°C. *Streptomyces* spores were harvested from MS solid medium (20 g l^{-1} soya flour, 20 g l^{-1} D-mannitol, 20 g l^{-1} agar) to count or inoculate. Plasmid DNA was transferred from ET12567/pUZ8002 to S*treptomyces* strain on M-ISP_4 media (1 g l^{-1} yeast extract, 2 g l^{-1} tryptone, 5 g l^{-1} soluble starch, 5 g l^{-1} D-mannitol, 5 g l^{-1} soyal flour, 1 g l^{-1} NaCl, 0.1% salt mix, 2 g l^{-1} $(NH4)_2SO_4$, 1 g l^{-1} K_2HPO_3, 2 g l^{-1} $CaCO_3$, 20 g l^{-1} agar, pH 7.0) following the reported procedures (Kieser *et al*., 2000). Random six exconjugants were separately picked and streaked on R2YE plates supplemented with 25 μg ml^{-1} apramycin and 25 μg ml^{-1} nalidixic acid. After 7 days, the genome DNA of each exconjugant was harvested to perform PCR evaluation. The recombinant plasmids pCM2-*dptP* or pSET152-*kasO*p*-*dptP* were respectively transferred from *E. coli* ET12567/pUZ8002 into *S. roseosporus* strain to obtain the *dptP*-deletion (ΔdptP) or *dptP*-overexpression (OP) strain. Growth rate was quantified by a simplified diphenylamine colorimetric method (Zhao *et al*., 2013). In this assay, DNA was hydrolysed into various components when exposed to the hot acidic conditions. Next, one of the components, deoxyriboses, were oxidized into 5-hydroxy-4 oxopentanals, which were then dimerized and condensed with diphenylamine to form the final products with typical absorbance at 595 nm.

To detect strain growth tolerance to DAP treatment, 1×10^7 spores of *S. roseosporus* or *S. ambofaciens* were inoculated in MYG containing DAP with a final concentration of 0-2 mg ml^{-1}. The growth rate was measured at 1–6 day. The experiment was performed three independent biological replicates.

Experimental design and statistical rationale

All *Streptomyces* strains used for transcription and protein analyses were cultivated in 30°C for 48 h. For measurement of growth rate and DAP tolerance, three independent experiments were performed, and the results based on Student's *t*-tests were shown as mean values (± standard deviation, SD). For LFQ proteomics analyses, three biological replicates and three technical replicates were performed for both WT and ΔdptP groups. In total, 18 raw data files were generated. WT group was set as control group. Proteins that were identified in more than two out of three technical replicates in at least one group were used for comparison. Student's *t*-tests (pairwise comparisons) were performed for comparisons between WT and ΔdptP groups, statistical analyses of abundance differences based on a cut-off of $P < 0.05$ on the post-imputated dataset, $P < 0.05$ were considered statistically significant.

LC- MS/MS identification

The WT and ΔdptP strain mycelia were cultured in 50 ml MYG at 30°C for 48 h. Mycelia pellets were collected to extract proteins using extraction buffer (50 mM Tris–HCl (pH 8.0), 0.2 mM ethylene diaminetetraaceticacid, 100 mM NaCl, and 1% (v/v) Triton X-100, 1% deoxycholate, 0.1% SDS).

Protein digestion was conducted according the FASP approach protocol (Wisniewski *et al*., 2009). A total of 200 μg proteins were treated with a final concentration of 50 mM dithiothreitol and then incubated at 50°C for 30 min. The proteins were diluted to 200 μl UA buffer (8 M urea in 50 mM Tris–HCl pH 8.1), and subsequently loaded to Amicon Ultra-15 Centrifugal Filters Ultracel-10 K (Merck Millipore, Ireland) which were pre-treated with 100 mM NaOH. 200 μl UA buffer was used to wash the proteins. Next, the proteins were treated with 100 μl 50 mM iodoacetamide diluted in UA buffer and incubated at 37°C in the dark. After that, 200 μl 50 mM ammonium bicarbonate was used to wash the proteins for two times. Next, proteins were digested with 2 μg sequencing-grade trypsin at 37°C for 16-18 h. Desalting was processed using C18-SD extraction disc (2215, 3M, MN).

The desalted peptide mixtures were analysed by LC-MS/MS on an easy nano-LC1000 HPLC system (Thermo Scientific, San Jose, CA) and a Q-Exactive mass spectrometer (Thermo Scientific, San Jose, CA). Peptides were loaded onto a trap column (Thermo Scientific Acclaim PepMap 100, 100 μm × 2 cm, nanoViper C18) from automatic with a mobile phase A, 0.1 % formic acid, and a mobile phase B, 0.1% acidic mixture (84% acetic acid, 16% acetonitrile). Samples were separated by a nano-analytical column (Thermo scientific EASY column, 10 cm, 75 μm, 3 μm, C18-A2) at a flow rate of 300 nl min^{-1}. Survey scan ranges 300–1800 *m/z* at a resolution of 70 000. Isolation window was acquired at a resolution of 17 500 with an isolation window of 1.6 *m/z*. The MS/MS scans were performed at a resolution of 17 500. The target value for the full MS scan was 1×10^6 with a maximum injection time of 20 ms, and that for the MS/MS scan was 1×10^5 with a maximum injection time of 100 ms.

For MS/MS detection, the mass to charge ratio (*m/z*) of the peptide fragment was detected. The fragmentation of peptide segments in mass spectrometry has a certain regularity. The parent ion of peptide is dissociated by high energy collision dissociation (HCD) or collision-induced dissociation (CID). The peptide chain breaks off at C-N bond (HCD) or C-C bond (CID) and forms daughter ions. Then, b, y (HCD) and a (CID) ions are generated. HCD was applied in this study. According to these y and b ions, the amino acid sequences can be calculated.

Analyses for MS data

A total of 18 raw files generated from LC-MS/MS were analysed via MaxQuant search engine (Lin *et al*., 2019) (version 1.6.0.16). Based on the MaxQuant search engine, the LC–MS/MS data were searched against the Uniprot database restricted to *S. roseosporus* which contains 6520 sequences (Nov 29th, 2019). Two missed tryptic cleavages were allowed. Oxidation (M) and protein N-terminal acetylation (N) were allowed to be the variable modifications, and carbamidomethylation of cysteine was allowed to be a fixed modification. Initial peptide mass tolerance was set to 20 ppm and fragment mass tolerance was 0.1 Da. + 2 was set as default charge state of each peptide. The false discovery rates (FDRs) of peptide and protein were set as 0.01. LFQ min ratio count was set as 2.

Perseus (version 1.6.1.3) was used to analyse clustering and correlation (Lin *et al*., 2019). The invalid values caused by contaminants and peptides identified by site were filtered by default setting in Perseus. Additionally, LFQ intensities were generated using log (base 2) transformation. Each sample was assigned to its corresponding group, WT (control) versus ΔdptP. At least two unique peptides of a protein successfully detected in each sample was acceptable. The proteins identified in more than two out of three biological replicates in at least one group were used for further analyses. A data imputation step was used to replace the missing values with values of low abundant proteins. These proteins were randomly chosen from a distribution specified by a downshift of 1.8 times the mean SD of all measured values and a width of 0.3 times this SD. The two-sample *t*-tests were conducted based on normalized intensity values. The absent proteins in one group were identified from the pre-imputation dataset. GO and KEGG analyses were carried out in KEGG database. *t*-Tests were used to compare difference of two groups. Zscores was used to count the enrichment values of the pathways (Liu *et al*., 2020).

Extraction and identification of membrane proteins

Total proteins were extracted using lysis buffer (50 mM Tris–HCl, pH 8.0, 0.2 mM EDTA, 100 mM NaCl, and 1% (v/v) Triton X-100, 1% deoxycholate, 0.1% SDS). The detergent triton X-100 and SDS improved the extraction efficiency of membrane protein. Extraction of membrane proteins was referred to the previous report (Cheng and Li, 2014). For separation of membrane from cytoplasm, mycelia were lysed using lysis buffer 1 (50 mM Tris–HCl (pH 7.5), 150 mM NaCl, 1 mM phenylmethanesulfonyl fluoride (PMSF), 1 mM trichloroethyl phosphate (TCEP)) and centrifugated at 8000 g for 40 min. The supernatant was collected for high-speed centrifugation at 110 000 g for 1 h. The supernatant was collected for preparation of cytoplasm proteins, and the precipitate was resuspended using lysis buffer 2 (50 mM Tris–HCl (pH 7.4), 150 mM NaCl, 1% Triton X-100, 1% sodium deoxycholate, 1% NP-40, 1 mM PMSF) to collect membrane proteins. The cytoplasm and membrane fractions with equal mass were used to detect the localization of DptP by Western blot. Moreover, Flag-tagged DptP protein and its interacting proteins were enriched using anti-Flag antibody-coupled beads and separated using SDS-PAGE. Then, the target SDS-PAGE was cut and digested with trypsin followed by desalting and MS identification.

Gene transcription analysis

The WT, ΔdptP and OP strain mycelia were cultured in 3 ml MYG at 30°C for 48 h and then collected for total RNA extraction and subsequent transcription analysis. The transcription levels of *dpt* gene cluster members, including *dptA*, *dptBC*, *dptD*, *dptE*, *dptF*, *dptG*, *dptP*, *dptM*, *dptN*, *dptR1*, *dptR2* and *dptR3*, were measured by real time-quantitative PCR (RT-qPCR). The PCR reaction mix included 5 μl of SYBR Green Mix, 1 μl of cDNA, 1 μl of each primer at a final 10 pmol ml^{-1} concentration and 5 μl of ddH_2O. The endogenous gene *hrdB*, encoding a RNA polymerase sigma factor, was used as the internal control. The expression levels of target genes were normalized by the expression of *hrdB*. The experiment was performed at least three independent biological replicates.

Western blot analysis

Protein quantification was performed using BCA protein assay kit (P0012; Beyotime Biotechnology, Shanghai, China). Western blot analysis was performed following the procedures as previously described (Zhang *et al*., 2017). 60 μg proteins of each group were separated using SDS-PAGE. Western blot analysis was performed with rabbit polyclonal anti-Flag antibody (0912-1; Huabio, Hangzhou, Zhejiang, China).

Acknowledgements

This work was financially supported by the grants from Sichuan Science & Technology Program (2020YFH0094), Chengdu Science & Technology Program (2020-GH02-00056-HZ) and the Health Commission of Sichuan Province (17ZD045). We also acknowledged Yi Zhong assistant researcher from the Frontiers Science Center for Disease-related Molecular Network, Institutes for Systems Genetics, West China Hospital of Sichuan University, for identification of DptP-interacting proteins by MS.

Conflict of interests

The authors declare that they have no competing interests.

Authors' contributions

Dan Zhang, Xixi Wang, Yang Ye, Yu He performed experiments. Fuqiang He and Yongqiang Tian analyzed data. Yunzi Luo supervised *dptP*-deletion plasmid construction. Shufang Liang conceived, instructed experiments and revised the paper. All authors read and approved the final manuscript.

References

Acharya, D., Miller, I., Cui, Y., Braun, D.R., Berres, M.E., Styles, M.J., *et al*. (2019) Omics technologies to understand activation of a biosynthetic gene cluster in *Micromonospora* sp. WMMB235: Deciphering keyicin biosynthesis. *ACS Chem Biol* **14:** 1260–1270.

Akins, R.L., and Rybak, M. J. (2001) Bactericidal activities of two daptomycin regimens against clinical strains of glycopeptide intermediate-resistant *Staphylococcus aureus*, vancomycin-resistant *Enterococcus faecium*, and methicillin-resistant *Staphylococcus aureus* isolates in an *in vitro* pharmacodynamic model with simulated endocardial vegetations. *Antimicrob Agents Chemother* **45:** 454–459.

Alexander, D., Davies, J., Miao, V., and Baltz, R. H. (2004) *Genetics and molecular biology for industrial microorganisms/biotechnology of microbial Products (GMBIM/BMP)*, abstract P5, SanDiego, CA, November 14–18, 2004.

Arbeit, R.D, Maki, D., Tally, F.P., Campanaro, E., and Eisenstein, B.I. (2004) The safety and efficacy of daptomycin for the treatment of complicated skin and skin-structure infections. *Clin Infect Dis* **38:** 1673–1681.

Baltz, R.H. (2008) Biosynthesis and genetic engineering of lipopeptide antibiotics related to daptomycin. *Curr Top Med Chem* **8:** 618–638.

Baltz, R.H., Miao, V., and Wrigley, S.K. (2005) Natural products to drugs: daptomycin and related lipopeptide antibiotics. *Nat Prod Rep* **22:** 717–41.

Bierman, M., Logan, R., O'Brien, K., Seno, E.T., Rao, R.N., and Schoner, B.E. (1992) Plasmid cloning vectors for the conjugal transfer of DNA from *Escherichia Coli* to *Streptomyces* spp. *Gene* **116:** 43–49.

Boll, B., Taubitz, T., and Heide, L. (2011) Role of MbtH-like proteins in the adenylation of tyrosine during aminocoumarin and vancomycin biosynthesis. *J Biol Chem* **286:** 36281–36290.

Bordoloi, N.K., Bhagowati, P., Chaudhuri, M.K., and Mukherjee, A.K. (2016) Proteomics and metabolomics analyses to elucidate the desulfurization pathway of *Chelatococcus* sp. *PLoS One* **11:** e0153547.

Boughner, L.A., and Doerrler, W.T. (2012) Multiple deletions reveal the essentiality of the DedA membrane protein family in *Escherichia coli*. *Microbiology* **158:** 1162–1171.

Butler, M.S., Robertson, A.A., and Cooper, M.A. (2014) Natural product and natural product derived drugs in clinical trials. *Nat Prod Rep* **31:** 1612–1661.

Chen, B., Zhang, D., Wang, X., Ma, W., Deng, S., Zhang, P., *et al*. (2017) Proteomics progresses in microbial physiology and clinical antimicrobial therapy. *Eur J Clin Microbiol Infect Dis* **36:** 403–413.

Cheng, W., and Li, W. (2014) Structural insights into ubiquinone biosynthesis in membranes. *Science* **343:** 878–81.

Cobb, R.E., Wang, Y., and Zhao, H. (2015) High-efficiency multiplex genome editing of *Streptomyces* species using an engineered CRISPR/Cas system. *ACS Synth Biol* **4:** 723–728.

Davidsen, J.M., Bartley, D.M., and Townsend, C.A. (2013) Non-ribosomal propeptide precursor in nocardicin a biosynthesis predicted from adenylation domain specificity dependent on the MbtH family protein NocI. *J Am Chem Soc* **135:** 1749–1759.

Debono, M., Barnhart, M., Carrell, C.B., Hoffmann, J.A., Occolowitz, J.L., Abbott, B.J., *et al*. (1987) A21978C, a complex of new acidic peptide antibiotics: Isolation, chemistry, and mass spectral structure elucidation. *J Antibiot (Tokyo)* **40:** 761–777.

Doerrler, W.T., Sikdar, R., Kumar, S., and Boughner, L.A. (2013) New functions for the ancient DedA membrane protein family. *J Bacteriol* **195:** 3–11.

Fluman, N., Ryan, C.M., Whitelegge, J.P., and Bibi, E. (2012) Dissection of mechanistic principles of a secondary multidrug efflux protein. *Mol Cell* **47:** 777–787.

Gubbens, J., Zhu, H., Girard, G., Song, L., Florea, B.I., Aston, P., *et al*. (2014) Natural product proteomining, a quantitative proteomics platform, allows rapid discovery of biosynthetic gene clusters for different classes of natural products. *Chem Biol* **21:** 707–718.

Guo, M., Zhang, X., Li, M., Li, T., Duan, X., Zhang, D., *et al*. (2019) Label-free proteomic analysis of molecular effects of 2-methoxy-1,4-naphthoquinone on penicillium italicum. *Int J Mol Sci* **20:** 3459.

Holdsworth, S.R., and Law, C.J. (2012) Functional and biochemical characterisation of the *Escherichia coli* major facilitator superfamily multidrug transporter MdtM. *Biochimie* **94:** 1334–1346.

Ke, J., and Yoshikuni, Y. (2019) Multi-chassis engineering for heterologous production of microbial natural products. *Curr Opin Biotechnol* **62:** 88–97.

Keller, R., and Schneider, D. (2013) Homologs of the yeast Tvp38 vesicle-associated protein are conserved in chloroplasts and cyanobacteria. *Front Plant Sci* **4:** 467.

Kieser, T., Bibb, M.J., Buttner, M.J., Chater, K.F., and Hopwood, D.A. (2000) *Practical Streptomyces* Genetics. Norwich, UK: John Innes Foundation.

Kumar, S., and Doerrler, W.T. (2014) Members of the conserved DedA family are likely membrane transporters and are required for drug resistance in *Escherichia coli*. *Antimicrob Agents Chemother* **58:** 923–930.

Kumar, S., and Doerrler, W.T. (2015) *Escherichia coli* YqjA, a member of the conserved DedA/Tvp38 membrane protein family, is a putative osmosensing transporter required for growth at alkaline pH. *J Bacteriol* **197:** 2292–3000.

Li, J., Long, X., Hu, J., Bi, J., Zhou, T., Guo, X., *et al*. (2019) Multiple pathways for natural product treatment of

Parkinson's disease: a mini review. *Phytomedicine* **60:** 152954.
Lin, Y.H., Eguez, R.V., Torralba, M.G., Singh, H., Golusinski, P., Golusinski, W., *et al*. (2019) Self-assembled STrap for global proteomics and salivary biomarker discovery. *J Proteome Res* **18:** 1907–1915.
Liu, J., Huang, Z., Ruan, B., Wang, H., Chen, M., Rehman, S., and Wu, P. (2020) Quantitative proteomic analysis reveals the mechanisms of polymyxin B toxicity to *Escherichia coli*. *Chemosphere* **259:** 127449.
Machado, H., Tuttle, R.N., and Jensen, P. R. (2017) Omics-based natural product discovery and the lexicon of genome mining. *Curr Opin Microbiol* **39:** 136–142.
Mao, X.M., Luo, S., Zhou, R.C., Wang, F., Yu, P., Sun, N., *et al*. (2015) Transcriptional regulation of the daptomycin gene cluster in *Streptomyces roseosporus* by an autoregulator, AtrA. *J Biol Chem* **290:** 7992–8001.
Miao, V., Coeffet-Legal, M.F., Brian, P., Brost, R., Penn, J., Whiting, A., *et al*. (2005) Daptomycin biosynthesis in *Streptomyces roseosporus*: cloning and analysis of the gene cluster and revision of peptide stereochemistry. *Microbiology* **151:** 1507–1523.
Panta, P.R., Kumar, S., Stafford, C.F., Billiot, C.E., Douglass, M.V., Herrera, C.M., *et al*. (2019) A dedA family membrane protein is required for *Burkholderia thailandensis* colistin resistance. *Front Microbiol* **10:** 2532.
Robbel, L., and Marahiel, M.A. (2010) Daptomycin, a bacterial lipopeptide synthesized by a nonribosomal machinery. *J Biol Chem* **285:** 27501–27508.
Sujeet, K., and William, T.D. (2014) Members of the conserved DedA family are likely membrane transporters and are required for drug resistance in *Escherichia coli*. *Antimicrob Agents Chemother* **58:** 923–930.
Sun, C. F., Xu, W.F., Zhao, Q.W., Luo, S., Chen, X.A., Li, Y.Q., and Mao, X.M. (2020) Crotonylation of key metabolic enzymes regulates carbon catabolite repression in *Streptomyces roseosporus*. *Commun Biol* **3:** 192.
Tao, W., Yang, A., Deng, Z., and Sun, Y. (2018) CRISPR/Cas9-based editing of *Streptomyces* for discovery, characterization, and production of natural products. *Front Microbiol* **9:** 1660.
Toymentseva, A.A., Koryagina, A.O., Laikov, A.V., and Sharipova, M.R. (2020) Label-free multiple reaction monitoring, a promising method for quantification analyses of specific proteins in bacteria. *Int J Mol Sci* **21:4924.**
Wang, Y., Cobb, R.E., and Zhao, H. (2016) High-efficiency genome editing of *Streptomyces* species by an engineered CRISPR/Cas system. *Methods Enzymol* **575:** 271–284.
Wang, W., Li, X., Wang, J., Xiang, S., Feng, X., and Yang, K. (2013) An engineered strong promoter for *Streptomycetes*. *Appl Environ Microbiol* **79:** 4484–4492.
Wang, F., Ren, N.N., Luo, S., Chen, X.X., Mao, X.M., and Li, Y.Q. (2014) DptR2, a DeoR-type auto-regulator, is required for daptomycin production in *Streptomyces roseosporus*. *Gene* **544:** 208–215.
Wisniewski, J.R., Zougman, A., Nagaraj, N., and Mann, M. (2009) Universal sample preparation method for proteome analysis. *Nat Methods* **6:** 359–362.
Wittmann, M., Linne, U., Pohlmann, V., and Marahiel, M.A. (2008) Role of DptE and DptF in the lipidation reaction of daptomycin. *FEBS J* **275:** 5343–5354.
Xu, M., and Wright, G.D. (2019) Heterologous expression-facilitated natural products' discovery in actinomycetes. *J Ind Microbiol Biotechnol* **46:** 415–431.
Ye, Y., Xia, Z., Zhang, D., Sheng, Z., Zhang, P., Zhu, H., *et al*. (2019) Multifunctional pharmaceutical effects of the antibiotic daptomycin. *Biomed Res Int* **2019:** 8609218.
Zhang, Q., Chen, Q., Zhuang, S., Chen, Z., Wen, Y., and Li, J. (2015) A MarR family transcriptional regulator, DptR3, activates daptomycin biosynthesis and morphological differentiation in *Streptomyces roseosporus*. *Appl Environ Microbiol* **81:** 3753–3765.
Zhang, D., Xia, X., Wang, X., Zhang, P., Lu, W., Yu, Y., *et al*. (2017) PGRMC1 is a novel potential tumor biomarker of human renal cell carcinoma based on quantitative proteomic and integrative biological assessments. *PLoS One* **12:** e0170453.
Zhao, Y., Xiang, S., Dai, X., and Yang, K. (2013) A simplified diphenylamine colorimetric method for growth quantification. *Appl Microbiol Biotechnol* **97:** 5069–5077.
Zhu, F., Qin, C., Tao, L., Liu, X., Shi, Z., Ma, X., *et al*. (2011) Clustered patterns of species origins of nature-derived drugs and clues for future bioprospecting. *Proc Natl Acad Sci USA* **108:** 12943–12948.
Zhu, W., Smith, J.W., and Huang, C.M. (2010) Mass spectrometry-based label-free quantitative proteomics. *J Biomed Biotechnol* **2010:** 840518.
Zolova, O.E., and Garneau-Tsodikova, S. (2012) Importance of the MbtH-like protein TioT for production and activation of the thiocoraline adenylation domain of TioK. *MedChemComm* **3:** 950.

Supporting information

Additional supporting information may be found online in the Supporting Information section at the end of the article.

Fig. S1. The complete nucleotides of the 556-bp PCR fragment from *dptP*-deletion colony presented in Fig. 2C by DNA sequencing. The sequences presented in red font are 248-bp upstream genome sequences near *dptP*, and the sequences presented in blue font are 308-bp downstream sequences near *dptP*. The underlined sequences are the complete sequences of *dptP* gene. The deletion region includes these underlined sequences in black font.

Fig. S2. Label-free quantification (LFQ) proteomic analyses for differentially expressed proteins between *S. roseosporus* WT and ΔdptP strain. (A) Workflow of LFQ proteomics approach. (B) Venn diagram of proteins identified in WT and ΔdptP strains. 2076 proteins were initially identified in both WT and ΔdptP, 237 proteins were uniquely identified in WT. The multiscatter blot (C) and the cluster analysis (D) of the biological replicates indicated a high degree of similarity among the biological replicates. 1-3 represent the experimental and biological replicates of WT group; 4-6 represent the experimental and biological replicates of ΔdptP group

Fig. S3. The sequencing data of the 745-bp PCR product shows pSET152-*kasO*p*-*dptP* insertion into genomes of *S. roseosporus* and *S. ambofaciens*. The complete nucleotides of the Flag-tagging *dptP* amplified from the genome

DNA of *S. roseosporus* OP and *S. ambofaciens* harbouring pSET152-*kasO*p*-*dptP*. Nucleotide sequences of *kasO*p*, *dptP* and Flag tag were presented in red, black and purple font respectively.

Dataset S1. (A) All Proteins identified in WT. (B). All Proteins identified in ΔdptP group. (C) Statistically increased (*t*-test, $P < 0.05$) proteins in ΔdptP groupStatistically increased (*t*-test, $P < 0.05$) proteins in ΔdptP group. (D). Statistically decreased (*t*-test, $P < 0.05$) proteins in ΔdptP group. (E). Absent proteins in ΔdptP group.

Dataset S2. (A). Total DptP-interacting proteins.

Dataset S3. (A) Primers used in this study. (B) Strains and plasmids used in this study.